Title

Composition and Control of a Deg/ENaC Channel during Presynaptic Homeostatic Plasticity.

Journal

Cell reports, 20(8)

ISSN

2211-1247

Authors

Orr, Brian O
Gorczyca, David
Younger, Meg A
et al.

Publication Date

2017-08-01

DOI

10.1016/j.celrep.2017.07.074

Peer reviewed

Article

Cell Reports

Composition and Control of a Deg/ENaC Channel during Presynaptic Homeostatic Plasticity

Graphical Abstract

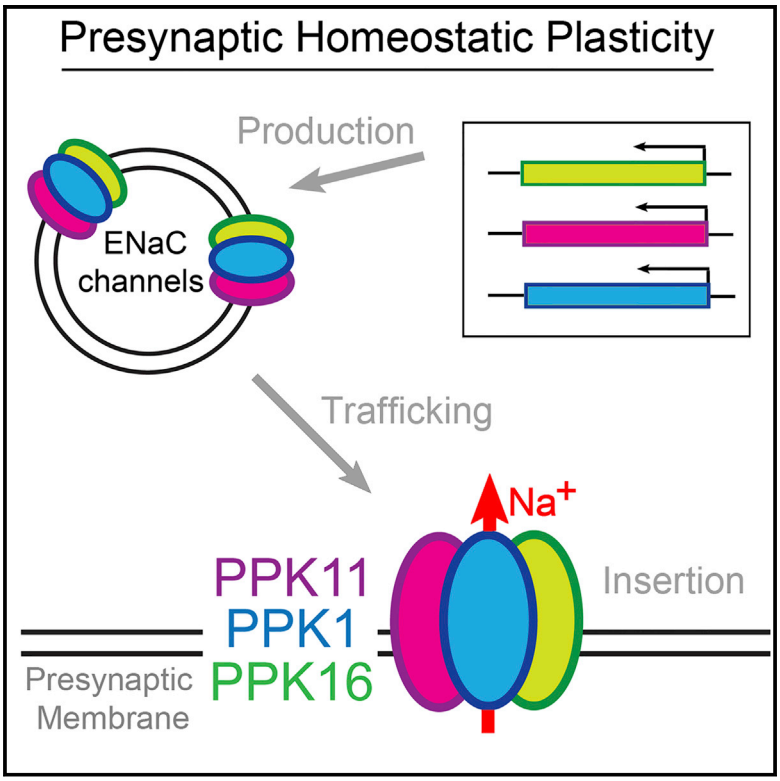

Authors

Brian O. Orr, David Gorczyca, Meg A. Younger, Lily Y. Jan, Yuh-Nung Jan, Graeme W. Davis

Correspondence

graeme.davis@ucsf.edu

In Brief

Orr et al. define the subunit composition of an essential Deg/ENaC channel that controls the rapid induction and sustained expression of presynaptic homeostatic plasticity. The demonstration that PPK1 incorporates into DEG/ENaC channels with diverse physiological activities highlights the potential for tremendous DEG/ENaC channel diversity in *Drosophila.*

Highlights

- The Deg/ENaC channel subunit PPK1 is essential for presynaptic homeostasis
- PPK1 functions in concert with PPK11/16 as a heterotrimeric Deg/ENaC channel
- Overexpressed PPK1-GFP distributes within the presynaptic nerve terminal
- PPK1 protein levels are controlled by the induction of presynaptic homeostasis

Orr et al., 2017, Cell Reports *20*, 1855–1866
August 22, 2017
http://dx.doi.org/10.1016/j.celrep.2017.07.074

CellPress

Cell Reports
Article

Composition and Control of a Deg/ENaC Channel during Presynaptic Homeostatic Plasticity

Brian O. Orr,[1] David Gorczyca,[2] Meg A. Younger,[1] Lily Y. Jan,[2] Yuh-Nung Jan,[2] and Graeme W. Davis[1,3,*]
[1]Department of Biochemistry and Biophysics, Kavli Institute for Fundamental Neuroscience, University of California, San Francisco, San Francisco, CA 94158, USA
[2]Howard Hughes Medical Institute, Department of Physiology, University of California, San Francisco, San Francisco, CA 94158, USA
[3]Lead Contact
*Correspondence: graeme.davis@ucsf.edu
http://dx.doi.org/10.1016/j.celrep.2017.07.074

SUMMARY

The homeostatic control of presynaptic neurotransmitter release stabilizes information transfer at synaptic connections in the nervous system of organisms ranging from insect to human. Presynaptic homeostatic signaling centers upon the regulated membrane insertion of an amiloride-sensitive degenerin/epithelial sodium (Deg/ENaC) channel. Elucidating the subunit composition of this channel is an essential step toward defining the underlying mechanisms of presynaptic homeostatic plasticity (PHP). Here, we demonstrate that the *ppk1* gene encodes an essential subunit of this Deg/ENaC channel, functioning in motoneurons for the rapid induction and maintenance of PHP. We provide genetic and biochemical evidence that PPK1 functions together with PPK11 and PPK16 as a presynaptic, heterotrimeric Deg/ENaC channel. Finally, we highlight tight control of Deg/ENaC channel expression and activity, showing increased PPK1 protein expression during PHP and evidence for signaling mechanisms that fine tune the level of Deg/ENaC activity during PHP.

INTRODUCTION

Homeostatic signaling systems stabilize neural function through the modulation of presynaptic transmitter release, ion channel abundance, and neurotransmitter receptor trafficking (Davis, 2013; Marder and Goaillard, 2006; Turrigiano, 2008). The homeostatic modulation of neurotransmitter release has been observed at mammalian central synapses (Kim and Ryan, 2010; Zhao et al., 2011) and at neuromuscular synapses in species ranging from *Drosophila* to mouse and human (Davis, 2013; Cull-Candy et al., 1980; Wang et al., 2016). In these systems, decreased neurotransmitter receptor sensitivity is precisely counteracted by a homeostatic potentiation of neurotransmitter release, thereby maintaining appropriate muscle excitation, a process termed presynaptic homeostatic plasticity (PHP) (Gaviño et al., 2015).

Core molecular components of the signaling systems that achieve PHP have begun to emerge through the results of large-scale forward genetic screens at the *Drosophila* neuromuscular junction (NMJ) (Brusich et al., 2015; Dickman and Davis, 2009; Müller et al., 2012, 2015; Wang et al., 2014; Younger et al., 2013) and additional hypothesis-driven studies (Penney et al., 2012). A core finding has been the demonstration that an amiloride-sensitive degenerin/epithelial sodium (Deg/ENaC) channel functions presynaptically to drive the induction and sustained expression of PHP (Younger et al., 2013). Presynaptic Deg/ENaC channel activity is not detected at baseline but is rapidly induced upon postsynaptic neurotransmitter receptor inhibition (Younger et al., 2013). A current model suggests that ENaC channel insertion causes a sodium leak that depolarizes the presynaptic membrane and subsequently potentiates calcium influx through active-zone-localized CaV2.1 calcium channels. This model is supported by a combination of ENaC channel pharmacology and presynaptic calcium imaging (Younger et al., 2013).

Deg/ENaC channels encompass a broad family of non-voltage-activated sodium and, in some instances, calcium-permeable channels that are believed to be heterotrimeric subunit assemblies (Anantharam and Palmer, 2007; Firsov et al., 1998; Kosari et al., 1998; Zelle et al., 2013). This family includes sodium leak channels (Chalfie, 2009), channels gated by low pH (Boiko et al., 2012; Du et al., 2014), chemoreceptors (Lin et al., 2005; Mast et al., 2014; Toda et al., 2012), and mechanoreceptors (Chen and Chalfie, 2015; Goodman et al., 2002; Gorczyca et al., 2014; Guo et al., 2014). Beyond this, a growing list of ligands has been shown to activate these channels, including small neuropeptides and opioid peptides (Askwith et al., 2000). Increasing evidence suggests that channel subunit composition determines the biophysical properties of the channel, as well as the intracellular trafficking and channel localization (Askwith et al., 2004; Sherwood et al., 2011; Zelle et al., 2013). Thus, defining the subunit composition of the ENaC channel that drives PHP is an essential step toward defining the feedback control mechanisms that govern the expression of PHP.

In *Drosophila*, there is the potential for tremendous Deg/ENaC channel heterogeneity. The *ppk* gene family encodes a diverse family of Deg/ENaC channel subunits, and with 31 independent *ppk* genes encoded in the genome, the combinatorial space for unique ion channel assemblies is tremendous (Zelle et al., 2013). To date, however, the full subunit composition of *Drosophila* Deg/ENaC channels with clearly defined biological activities has yet to be achieved, and therefore, very little is known about

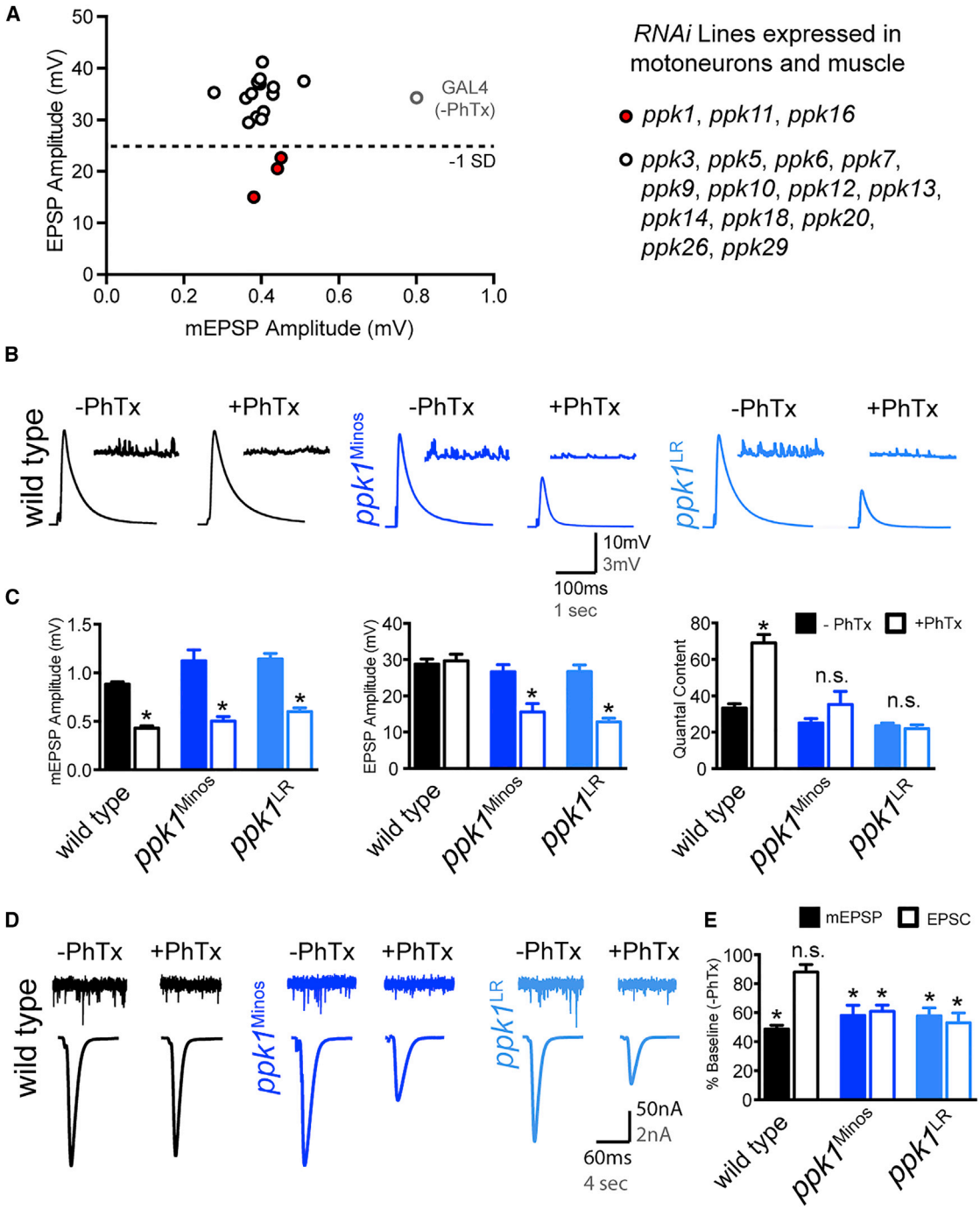

Figure 1. *ppk1* Is Required for Presynaptic Homeostatic Plasticity

(A) Data from a *UAS-RNAi* expression screen of *ppk* genes. Data are displayed in the presence of PhTx (open black circles) or the control genotype *GAL4* (open gray circle, in the absence of PhTx). Tested genotypes are listed, and those indicated in red have a mean EPSP that is more than 1 SD below the mean of all tested genotypes in the presence of PhTx (a threshold indicated by the horizontal dotted line).

(B) Representative traces for the indicated genotypes (0.3 mM extracellular calcium).

(C) Quantification of average mEPSP, EPSP, and QC. Neither ppk^{Minos} nor ppk^{LR} mutants exhibited a significant increase in QC in the presence of PhTx (n.s.; p = 0.19 and p = 0.56, respectively).

(D) Representative traces for indicated genotypes (1.5 mM extracellular calcium).

(legend continued on next page)

diversity and biological relevance of this large gene family. By screening a collection of *ppk-RNAi* transgenes, we have defined a third essential subunit of the Deg/ENaC channel that is required for PHP at the *Drosophila* NMJ. This subunit is encoded by the *ppk1* gene. This finding is a surprise, given that PPK1 participates in a very different type of channel in peripheral sensory neurons. In the DA sensory neurons, PPK1 functions with PPK26 as part of a highly expressed mechanotransduction channel (Gorczyca et al., 2014; Guo et al., 2014; Mauthner et al., 2014). The third subunit of the DA-neuron PPK1-containing mechanotransduction channel has yet to be identified, although it remains possible that the DA-neuron channel is not heterotrimeric (Chen et al., 2015). By characterizing a PPK1 containing ENaC channel in the context of PHP, we provide direct evidence that different PPK subunit assemblies can generate channels with very different properties and unique physiological roles in *Drosophila* neurons.

RESULTS

PPK1 Is Necessary for the Rapid Induction and Sustained Expression of Presynaptic Homeostatic Plasticity

We sought to identify the full subunit composition of the Deg/ENaC channel that controls PHP. In our experiments, PHP is induced by the application of a sub-blocking concentration (15 μM) of the glutamate receptor antagonist philanthotoxin (PhTx) (see Experimental Procedures). Application of PhTx has been repeatedly demonstrated to decrease miniature excitatory postsynaptic potential (mEPSP) amplitude and induce an offsetting, homeostatic increase in presynaptic release that restores EPSP amplitudes to wild-type values (Frank et al., 2006; Younger et al., 2013). First, we performed an RNAi-based screen of the *Drosophila ppk* genes. We expressed available transgenic *UAS-RNAi* directed against individual *ppk* genes, doing so simultaneously in motoneurons and muscle using a combination of two *GAL4* drivers in a single animal: *OK371-GAL4*, which expresses in motoneurons, and *BG57-GAL4*, which expresses in muscle. For each *UAS-ppk-RNAi* genotype, we quantified mEPSP amplitude, EPSP amplitude, quantal content (average mEPSP amplitude/EPSP amplitude), resting membrane potential (RMP), and input resistance (R_{in}) in the presence of PhTx. The results of this screen are presented in Figure 1A. Three RNAi lines were shown to block PHP in our screen. Two of these lines target expression of PPK11 and PPK16 (Figure 1A, red), previously shown to be required for PHP (Younger et al., 2013). The third hit was an RNAi targeting the expression of the *ppk1* gene. Thus, PPK1 is a strong candidate to be the third subunit of the Deg/ENaC channel necessary for PHP.

It is worth noting that our screen also included an RNAi directed against the *ppk18* gene. The *ppk18* gene resides adjacent to the *ppk11* and *ppk16* genes in the genome. It was previously shown that the *ppk11* and *ppk16* genes are transcribed as a single mRNA and both are necessary for PHP (Younger et al., 2013). However, we found no evidence that *ppk18* participates in PHP. This conclusion is based on our analysis of the *ppk18-RNAi* transgene driven by *OK371-GAL4* and is supported by an analysis of two loss-of-function mutations that specifically disrupt the *ppk18* gene locus (data not shown). Thus, whereas all three genes (*ppk11*, *ppk16*, and *ppk18*) reside adjacent to each other in the genome, only *ppk11* and *ppk16* participate in the ENaC channel required for PHP.

Next, we sought to confirm, genetically, that *ppk1* is necessary for PHP. To do so, we tested two independent mutations previously demonstrated to disrupt the *ppk1* gene. We examined a transposon insertion line, $ppk^{MI04968}$ (referred to as ppk^{Minos}), that resides in the 3′ UTR of the *ppk1* gene. We also tested a molecularly defined *ppk1*-null mutation (a small deletion that removes the entire gene) termed $ppk^{LargeRegion}$ (ppk^{LR}) (note that ppk^{LR} was originally published as $ppk1^{ESB}$ in Boiko et al., 2012). Here, we demonstrate that both ppk^{Minos} and ppk^{LR} completely block the rapid induction of PHP (Figures 1B and 1C; recordings in 0.3 mM extracellular [Ca^{2+}]. Note that sample sizes and additional values, including resting membrane potential and muscle input resistance, are presented in Table S1). Specifically, we demonstrate that application of PhTx to the NMJ causes a significant (~50%) decrease in mEPSP amplitude in each genotype (Figures 1B and 1C; $p < 0.01$; Student's t test comparing, within each genotype, the absence versus presence of PhTx). In wild-type (WT), following toxin application, there is a statistically significant, homeostatic increase in presynaptic quantal content (Figure 1C; $p < 0.01$). However, there is no change in quantal content in either ppk^{Minos} or ppk^{LR} (Figure 1C; $p > 0.1$ for each). As a consequence, EPSP amplitudes remain significantly smaller than control in ppk^{Minos} or ppk^{LR}, recorded in the presence of PhTx (Figure 1C). From these data, we conclude that *ppk1* is essential for the rapid induction of PHP.

We repeated the analysis of PHP at physiological extracellular calcium (1.5 mM $[Ca^{2+}]_e$), employing two-electrode voltage clamp to quantify AP-evoked excitatory postsynaptic currents (EPSCs). In each genotype, application of PhTx causes a significant decrease in mEPSP amplitude (Figures 1D and 1E; $p < 0.01$). Note that, as done previously (Müller et al., 2012, 2015), mEPSP amplitudes were used to assess the effectiveness of PhTx application prior to switching to two-electrode voltage clamp (TEVC). This is done because the signal to noise is far superior in the current clamp configuration compared to TEVC, allowing clear determination of the magnitude of the effect of PhTx on mEPSP amplitude. In both $ppk1^{Minos}$ and $ppk1^{LR}$, EPSC amplitudes remain significantly reduced by 40% compared to baseline in the absence of PhTx (Figures 1D and 1E; $p < 0.01$ for each

(E) Quantification of EPSCs for indicated genotypes in the presence of PhTx, normalized to baseline values recorded in the absence of PhTx for each genotype. If there were no changes in the presence of PhTx, values would remain at 100%. In wild-type, there is a significant PhTx-dependent decrease in mEPSP amplitude (asterisk; $p < 0.01$) but no significant percent decrease in EPSC amplitude compared to wild-type in the absence of PhTx (n.s; $p > 0.1$). Both ppk^{Minos} and ppk^{LR} mutants exhibited a significant decrease in mEPSP amplitudes and EPSC amplitudes in the presence of PhTx (asterisks; $p < 0.01$) compared to their own genotypic baseline in the absence of PhTx. Data are presented as average ± SEM. Comparisons within each genotype, comparing the presence versus absence of PhTx, were made using a Student's t test.

genotype comparing the presence versus absence of PhTx). Thus, PHP is blocked in $ppk1^{LR}$ at physiological extracellular calcium.

We note that the ppk^{LR} and $ppk1^{Minos}$ mutations have significant differences in baseline neurotransmission compared to wild-type. In these mutants, there is a significant increase in mEPSP amplitude compared to wild-type (Figure 1C; $p < 0.01$), no change in EPSP amplitudes compared to wild-type (Figure 1C; $p > 0.1$), and a significant reduction in quantal content compared to wild-type (Figure 1C; $p < 0.01$). Several points are worth emphasizing. First, the block in presynaptic homeostasis following loss of *ppk1* occurs whether or not there is a baseline decrease in quantal content. Specifically, expression of *UAS-ppk1-RNAi* in motoneurons blocks presynaptic homeostasis without a parallel change in mEPSP amplitude or quantal content ($p > 0.1$; see below for additional analyses of *UAS-ppk1-RNAi*). It is possible that *ppk1* has an additional postsynaptic function that influences baseline neurotransmission (see below for *ppk1* expression pattern). Second, the observation that quantal content is reduced in the ppk^{LR} mutation suggests that homeostatic depression of presynaptic release may have occurred to offset the observed increase in baseline mEPSP amplitude (Gaviño et al., 2015). The possible induction of homeostatic depression is unlikely to be the cause of impaired homeostatic potentiation because we recently demonstrated that PHP is unaffected by the prior induction of homeostatic depression (Gaviño et al., 2015).

PHP can also be induced by the genetic deletion of the nonessential *GluRIIA* subunit of the postsynaptic glutamate receptor, which causes a ~50% decrease in mEPSP amplitude. In this experiment, the NMJ lacks the GluRIIA subunit throughout larval development, and therefore, this experiment has been interpreted to reflect the sustained expression of PHP (Frank et al., 2006; Younger et al., 2013). We recombined the *ppk1*-null mutation (ppk^{LR}) with the *GluRIIA* mutation and quantified synaptic transmission (Figure 2). We find that the homeostatic potentiation of quantal content is blocked in the double mutant ($p > 0.1$, comparing ppk^{LR} to *GluRIIA*, ppk^{LR}). Thus, a second independent assay confirms that the *ppk1* gene is necessary for PHP. Taken together, we conclude that *ppk1* is essential for both the rapid induction and sustained expression of presynaptic homeostatic plasticity.

Finally, we asked whether impaired PHP is a secondary consequence of altered NMJ morphology. We stained the NMJ of wild-type and ppk^{LR} mutants using anti-horseradish peroxidase (HRP) to mark the presynaptic membrane, anti-Bruchpilot (Brp) to stain presynaptic active zones, and anti-Discs Large (Dlg) to label the postsynaptic muscle membranes (muscles 6/7). Qualitatively, there is no change in the appearance of the NMJ in ppk^{LR} ($n = 9$) compared to wild-type ($n = 9$; Figure 2D). Quantification of bouton number (abdominal segments 2 and 3) reveals no change ($p > 0.1$) in total bouton number at the NMJ comparing wild-type (158.89 ± 9.08) with ppk^{LR} (151.67 ± 13.53). There is also no difference in bouton number when comparing the type1b and type1s boutons between wild-type and ppk^{LR} (wild-type 1s = 80 ± 5.2; ppk^{LR} type 1s = 77 ± 8.8; $p > 0.4$, $n = 9$; wild-type 1b = 83 ± 5.7, ppk^{LR} 1b = 74 ± 15; $p > 0.5$, $n = 9$). Furthermore, quantification of active zone number (average number of Brp puncta per NMJ) demonstrates no change in this parameter ($p > 0.5$; $n = 9$) comparing wild-type (976.67 ± 56.13) with ppk^{LR} (1,027.33 ± 55.08). From these data, we conclude that impaired PHP in the *ppk1* mutant is not a secondary consequence of impaired anatomical NMJ development.

Elevated PPK1 Protein Levels during the Sustained Expression of PHP

A previously generated PPK1 antibody works well on western (Gorczyca et al., 2014) and has allowed us to determine whether PPK1 protein levels respond to the persistent induction of PHP. We assayed PPK1 protein levels by western blot, using the larval CNS as a tissue source. We find a significant increase in PPK1 protein levels in the *GluRIIA* mutant compared to controls (Figure 2B; $p < 0.01$). Thus, PPK1 protein is induced during long-term PHP. We propose that increased PPK1 protein is necessary to sustain the expression of PHP for prolonged periods of time. These data are consistent with previously published data demonstrating an ~400% increase in the transcription of the *ppk11* and *ppk16* genes during sustained PHP (Younger et al., 2013). However, it was never possible to generate antibodies to either PPK11 or PPK16. These data are evidence for enhanced protein expression for a presynaptic effector of PHP.

ppk1 Is Necessary in Motoneurons for the Expression of PHP

Using a combination of tissue-specific RNAi and genetic rescue, we demonstrate that *ppk1* is necessary in motoneurons for PHP. First, as a control, we demonstrate normal PHP in the heterozygous *OK371-GAL4* line following application of PhTx (Figures 3A–3C; $p < 0.05$). Next, when *UAS-ppk1-RNAi* is driven in motoneurons by *OK371-GAL4*, we show that PhTx-dependent PHP is blocked ($p > 0.1$, comparing *UAS-ppk1-RNAi/ OK371-GAL4* in the presence versus absence of PhTx). Furthermore, neither muscle-specific expression of *UAS-ppk1-RNAi* using *BG57-GAL4* nor trachea-specific expression of *UAS-ppk1-RNAi* with *btl-GAL4* had any effect on PHP, emphasizing a motoneuron-specific function of *ppk1* during PHP (see Table S1). Importantly, as noted above, neuronal expression of *UAS-ppk1-RNAi* does not alter baseline transmission but does block PHP. These data support the conclusion that *ppk1* has a specific role during PHP, separable from any effect on baseline neurotransmission that is observed in the *ppk1* mutant background.

Next, we performed genetic rescue of the ppk^{LR} mutant. We neuronally expressed a *UAS-ppk1-GFP* transgene in the PPK^{LR} mutant using the neuron-specific *C155-GAL4* driver. We find that PHP is fully rescued (Figures 3A–3C; $p < 0.01$ compared to baseline). We also performed genetic rescue using an endogenous *ppk1* promoter fragment fused to *ppk1-GFP* (1 kb fragment of the *ppk1* promoter; *ppk1>ppk1-GFP*; Gorczyca et al., 2014). Again, PHP is fully restored (Figures 3A–3C; *ppk1* promoter rescue; $p < 0.01$). These data, when combined with the results of motoneuron-specific RNAi, demonstrate that *ppk1* is endogenously expressed in motoneurons, where it functions to drive expression of PHP.

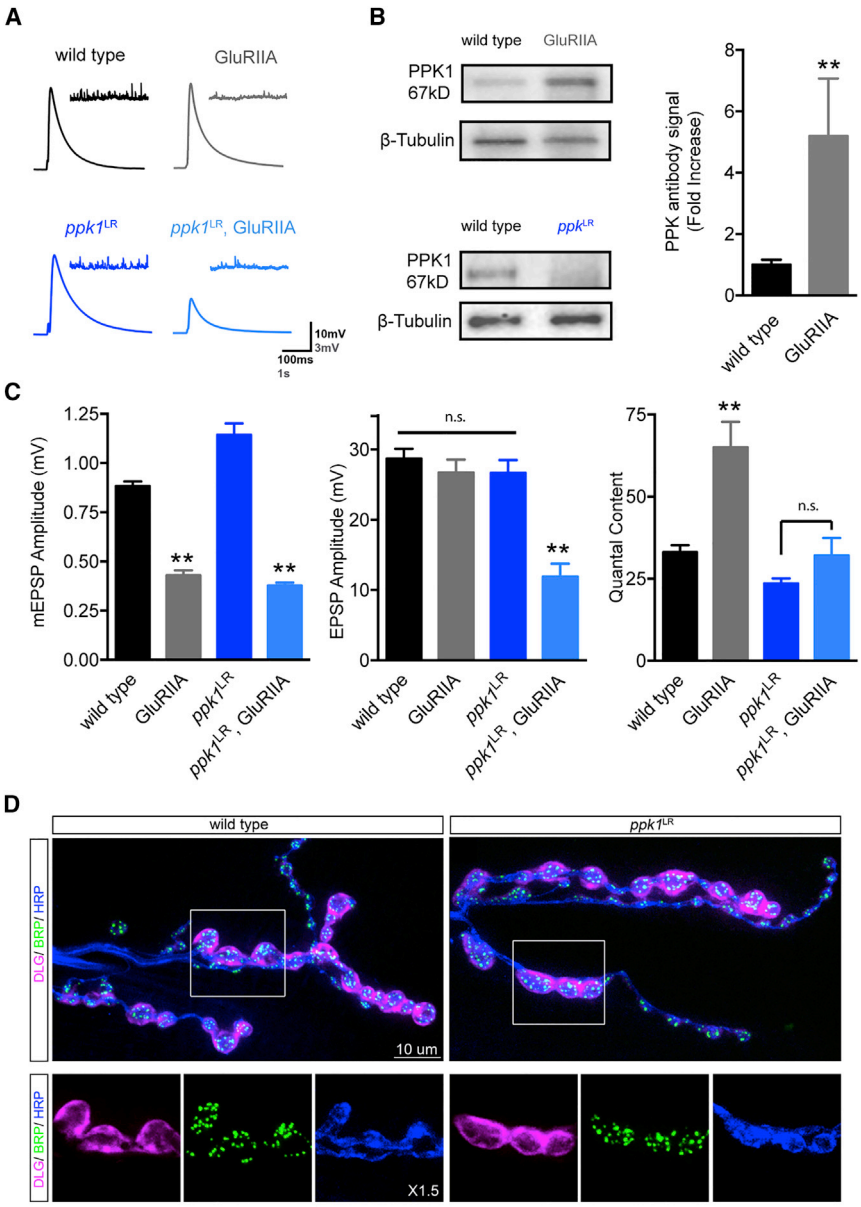

Figure 2. *ppk1* Is Required for the Sustained Expression of PHP

(A) Representative traces for the indicated genotypes (0.3 mM calcium).

(B) Quantification of PPK1 protein levels comparing wild-type with *GluRIIA*. The bottom two panels show the specificity of anti-PPK1 antibody. There is no band present in the PPk^{LR}-null mutant. Six biological replicates were performed, and total protein signal intensity was averaged. Data are presented as the average ± SEM. There is a significant increase in PPK1 protein in *GluRIIA* mutants ($p < 0.01$). Comparisons were made with Student's t test.

(C) Quantification of mEPSP, EPSP, and QC for the indicated genotypes. Average mEPSP amplitude is significantly reduced in the presence of the *GluRIIA* mutant ($p < 0.01$). The ppk^{LR}, *GluRIIA* double mutants do not show a significant increase in QC compared to ppk^{LR} mutants alone (n.s.; $p = 0.15$). Recordings were performed at 0.3 mM $[Ca^{2+}]_e$. Data are presented as average ± SEM. Comparisons (either wild-type to *GluRIIA* or ppk^{LR} to the ppk^{LR}, *GluRIIA* double mutant) were made with a Student's t test.

(D) The wild-type and ppk^{LR} NMJ stained with anti-HRP to label the presynaptic membrane (blue), anti-Brp to label the active zone (green), and anti-Dlg to label postsynaptic muscle membranes (magenta). The white box indicates the area shown at higher magnification below the indicated magnification. There were no significant differences observed comparing wild-type and ppk^{LR} mutants for 1s bouton number ($p = 0.41$; $n = 9$ for wild-type and ppk^{LR}), 1b bouton number ($p = 0.46$; $n = 9$ for wild-type and ppk^{LR}), total bouton number ($p = 0.28$; $n = 9$ for wild-type and ppk^{LR}), or active zone number ($p = 0.66$; $n = 9$ for wild-type and ppk^{LR}). Comparisons were made with a Student's t test.

Genetic and Biochemical Evidence that PPK1 Functions in Concert with PPK11 and PPK16 as Part of a Presynaptic Deg/ENaC Channel

We have pursued both genetic and biochemical evidence in support of the hypothesis that PPK1 functions with PPK11 and PPK16 as part of a heterotrimeric ENaC channel, necessary for PHP. First, we pursued genetic interaction experiments. Because each individual *ppk* gene mutation fully blocks PHP, without a profound effect on baseline transmission, a double mutant analysis is not informative. However, trans-heterozygous genetic interaction experiments have been used previously to implicate multiple homeostatic plasticity genes in a common presynaptic process (Younger et al., 2013; Harris et al., 2015; Wang et al., 2014). Here, we demonstrate that PHP is robustly expressed in the heterozygous $ppk1^{LR}$/+ mutant (Figures 4A and 4B). We then confirm that PHP is normal in animals harboring a small heterozygous deficiency that uncovers both the *ppk11* and *ppk16* genes (Younger et al., 2013). However, when we test animals harboring both a heterozygous ppk^{LR}/+ mutation and a heterozygous *ppk11-ppk16*/+ deficiency, we find that the homeostatic enhancement of presynaptic release is blocked (Figures 4A and 4B; $p > 0.1$). These data argue that the *ppk1* gene functions together with the *ppk11* and *ppk16* genes during PHP, potentially as subunits of a single Deg/ENaC channel. But biochemical evidence is necessary to confirm that all three proteins physically interact.

An antibody to PPK1 (Gorczyca et al., 2014) enabled us to test the physical interaction of the PPK1, PPK11, and PPK16 proteins in vivo. First, *UAS-ppk16-Venus* was co-expressed with *UAS-ppk11-FLAG* using a ubiquitous GAL4 driver (*actin-GAL4*; Figure 4D). We immunoprecipitated PPK16-Venus and tested for co-immunoprecipitation of both PPK11-FLAG and,

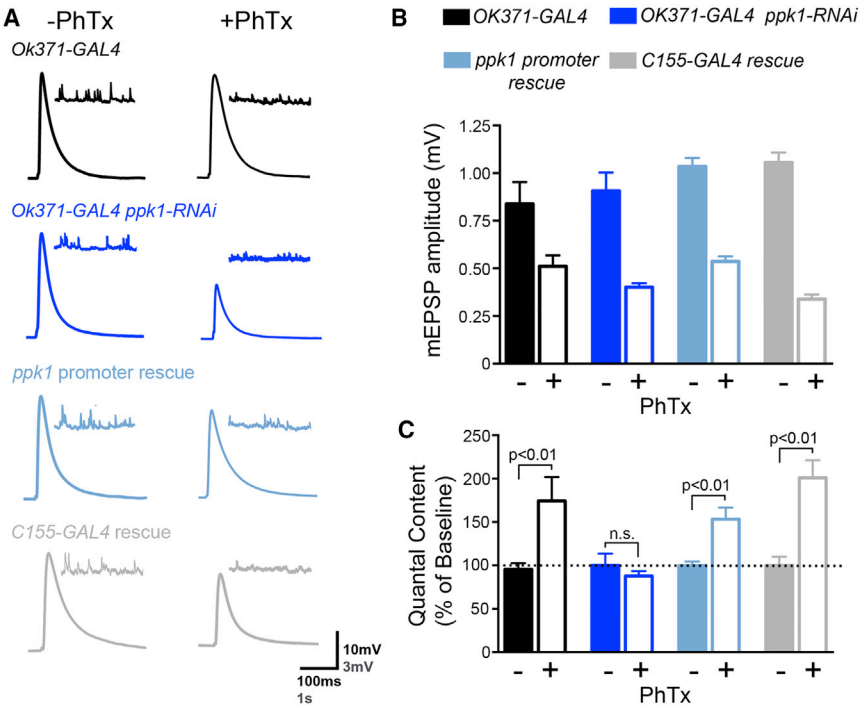

Figure 3. *ppk1* Is Required in Motoneurons for PHP

(A) Representative traces for the indicated genotypes, 0.3 mM $[Ca^{2+}]_e$.

(B) Quantification of average mEPSP and QC in the absence (−PhTx) and presence (+PhTx) of PhTx.

(C) Quantification of average quantal content (QC) in the absence (-PhTx) and presence (+PhTx) of PhTx. In control (*OK371-GAL4*/+), QC is significantly increased in the presence of PhTx ($p < 0.01$). Motoneuron-specific expression (*OK371-GAL4*/+) of *UAS-ppk1-RNAi* prevents a homeostatic increase in QC in the presence of PhTx (n.s.; $p = 0.16$). QC is significantly increased in the ppk^{LR} mutant when a *ppk1-GFP* transgene was expressed under the control of the endogenous *ppk1* promoter fragment ($p < 0.01$; *ppk1* promoter rescue). Rescue of PHP is also observed when *UAS-ppk1-GFP* expression is driven by the neuron-specific *C155-GAL4* ($p < 0.01$). Recordings were performed at 0.3 mM $[Ca^{2+}]_e$. Data are presented in average ± SEM. Comparisons (±PhTx for a given genotype) were made with a Student's t test.

independently, PPK1. We find that PPK16-Venus efficiently co-immunoprecipitates both PPK11 and PPK1, consistent with a physical interaction of these three ENaC channel subunits (Figure 4D). We then confirmed the specificity of this pull-down experiment by doing it in reverse. We immunoprecipitated endogenous PPK1 with the PPK1 antibody and demonstrate efficient co-immunoprecipitation of both PPK11-FLAG and PPK16-Venus (Figure 4E). Note that, each time we performed this experiment, we observed that the PPK1 antibody pulled down a background band that is immunoreactive with the FLAG antibody. This band is present in every control condition, even in the absence of the *UAS-ppk16-Venus* or *UAS-ppk11-FLAG* transgenes. Thus, this background band is not specific to our inquiry. Finally, we performed a third test of this interaction. Instead of using the PPK1 antibody, we repeated the triple pull-down experiment using a third transgene, an alpha-bungarotoxin binding site tagged *ppk11* transgene (*UAS-ppk11-αBt*). We co-expressed *UAS-ppk16-Venus*, *UAS-ppk1-FLAG*, and *UAS-ppk11-αBt* using *actin-GAL4*. Once again, we demonstrate that PPK1-FLAG co-immunoprecipitates both PPK11-αBt and PPK16-Venus (Figure 4C). Taken together with our functional genetic interaction data, these biochemical experiments argue strongly that PPK1 is part of a heterotrimeric Deg/ENaC channel that is essential for the expression of PHP.

PPK1 Is Acutely Required for the Expression of PHP

To this point, our data support the conclusion that PPK1 is part of a heterotrimeric Deg/ENaC channel that is necessary for PHP. If so, then the *ppk1* locus should be required for the pharmacological sensitivity of PHP to the ENaC channel antagonist benzamil. At the wild-type NMJ, benzamil (50 μm) blocks the expression of PHP, and this effect requires both the *ppk11* and the *ppk16* genes (Younger et al., 2013). First, we confirmed that the expression of PHP is blocked by benzamil application following the induction of PHP (Figure 5). We then demonstrate that the $ppk1^{LR}$ mutant does not express PHP and is insensitive to any further action of benzamil (Figure 5). We then demonstrate that motoneuron-specific rescue of the $ppk1^{LR}$ mutant with *UAS-ppk1-GFP* not only restored PHP but restores the benzamil sensitivity of presynaptic release. These data are further evidence that PPK1 functions acutely as a required third subunit of the presynaptic Deg/ENaC channel necessary for PHP.

PPK1 Protein Traffics to the Presynaptic Terminal

Previously published data argued that the Deg/ENaC channel that controls PHP is likely to localize at or near the nerve terminal, but there has been no histological evidence to support channel localization at this site. First, we drove *ppk1-GFP* under the control of the endogenous *ppk1* promoter (*ppk1>ppk1-GFP*). This condition reveals muscle, trachea, and nerve terminal PPK1 staining in the ppk^{LR} mutant background (Figure 6A). In this experiment, PPK1 puncta can be clearly observed in the motoneuron cell body and presynaptic boutons (Figure 6B). However, PPK1 staining in the trachea and muscle overlap with the NMJ, making it difficult to clearly assess protein distribution at the NMJ, consistent with the existence of other PPK subunits expressed in muscle (Hill et al., 2017). Therefore, we overexpressed *UAS-ppk1*-GFP presynaptically (*C155-GAL4*) in the ppk^{LR} mutant background and stained with the anti-GFP antibody to increase signal intensity. Because this transgene rescues PHP in the ppk^{LR} mutant background, the distribution of overexpressed presynaptic PPK1 protein should reflect, at least in part, the endogenous protein localization. We find that presynaptic PPK1-GFP resides in small puncta that are distributed at

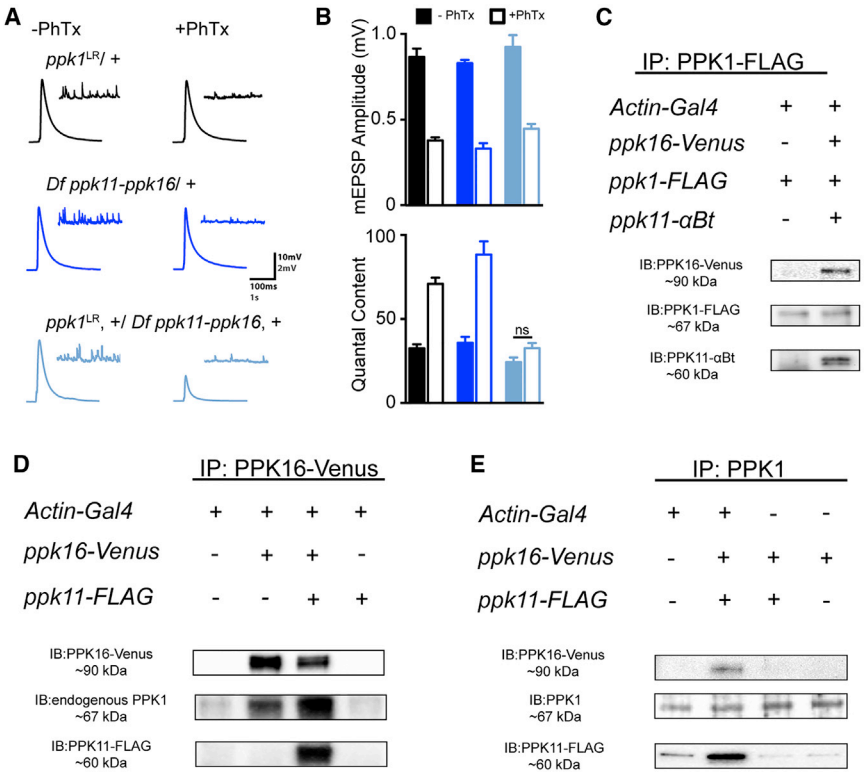

Figure 4. Genetic and Biochemical Interactions of PPK1, PPK11, and PPK16

(A) Representative mEPSP and EPSP traces from indicated genotypes in the absence and presence of PhTx. Recordings were performed at 0.3 mM $[Ca^{2+}]_e$.

(B) Averaged mEPSP and quantal content for genotypes in (A). In all genotypes, mEPSP amplitudes were reduced by ~50% in the presence of PhTx ($p < 0.01$; Student's t test). Heterozygous mutations (*ppk1*/+ and a double heterozygous mutant for *ppk11*/+ and *ppk16*/+) do not disrupt PHP, and an increase in quantal content is observed.

(C) Transgenes for *ppk16*-Venus, *ppk1*-Flag, and *ppk11*-αBt were co-expressed in *Drosophila* larvae under the control of actin-Gal4. PPK1-Flag co-immunoprecipitates PPK16-Venus and PPK11-αBt, when co-expressed.

(D) Transgenes for *ppk16*-Venus and *ppk11*-Flag were co-expressed in *Drosophila* larvae under the control of actin-Gal4. PPK16-Venus co-immunoprecipitates endogenous PPK1 and transgenically expressed PPK11-Flag.

(E) Transgenes for *ppk16*-Venus and *ppk11*-Flag were co-expressed in *Drosophila* larvae under the control of actin-Gal4. Using a PPK1 antibody, endogenous PPK1 co-immunoprecipitates transgenically expressed PPK16-Venus and PPK11-Flag. A non-specific band is present in all lanes (see text for additional commentary).

Data are presented as average ± SEM.

the bouton periphery, at or near the presynaptic plasma membrane delineated by anti-HRP (Figure 6C). All images are single confocal slices rather than Z projections of an image stack. We then assessed co-localization of PPK1 puncta with the active zone marker anti-Brp (Figure S1). We find that PPK1 puncta reside in close proximity to many, but not all, Brp puncta and there is no indication of protein co-localization. Taken together, these data support the conclusion that *ppk1* is endogenously expressed in muscle, trachea, and motoneurons. Our data confirm that PPK1 is present within the presynaptic nerve terminal, where it could reasonably function as a required subunit of the ENaC channel that includes PPK11 and PPK16.

PPK1 Is Required for the Homeostatic Expansion of the Readily Releasable Pool of Synaptic Vesicles

Although it has been clearly demonstrated that the size of the readily releasable pool of vesicles (RRP) scales sub-linearly with the concentration of extracellular calcium at both mammalian (Thanawala and Regehr, 2013) and *Drosophila* synapses (Müller et al., 2015), it has never been determined whether the ENaC-dependent change in presynaptic calcium influx that occurs during PHP is responsible, in part, for the expansion of the readily releasable pool of vesicles that is also observed during PHP. We now connect the dots.

We measured the RRP of the *ppk1*-null mutant (±PhTx). Measurement of the RRP was calculated following repetitive nerve stimulation of 60 Hz (30 stimuli) at 1.5 mM Ca^{2+} according to published methods (Schneggenburger et al., 1999; Müller et al., 2015). When PhTx is applied to the wild-type NMJ, we observe an expansion of the RRP (Figures 7A and 7B). Specifically, the measured cumulative EPSC is maintained at a constant level despite the significant reduction of mEPSP amplitudes by ~50%. When this experiment is repeated in the $ppk1^{LR}$-null mutant, the cumulative EPSC is decreased in proportion to the ~50% decrease in mEPSP amplitude caused by PhTx application. As a consequence, there is no expansion of the estimated RRP in this mutant. Thus, a PPK presynaptic ENaC channel is not only necessary for a PHP-dependent increase in presynaptic calcium influx (Younger et al., 2013) but is also required for the subsequent expansion of the readily releasable vesicle pool. These data serve to unify several observations in the field and define the PPK1/PPK11/PPK16-containing presynaptic ENaC channel as a core mechanism responsible for PHP.

Loss of PPK1 Causes and Age-Dependent Decline in Motor Function

Currently, there is very little information about whether PHP participates in behavioral, age-related motor decline. To address this, we assessed lifespan comparing wild-type controls to the $PPK1^{LR}$ mutant and find that there is not a dramatic change (G.W.D., unpublished data). Next, to assess an age-dependent decline in motor function, we assayed negative geotaxis, which is a strong innate behavior in *Drosophila* (Figure S2). We chose to assess negative geotaxis at two time points, one day after adult eclosion and 30 days after eclosion. The 30-day time point was chosen because it is approximately mid-lifespan for both wild-type and PPK^{LR} when raised at 25°C. It has been

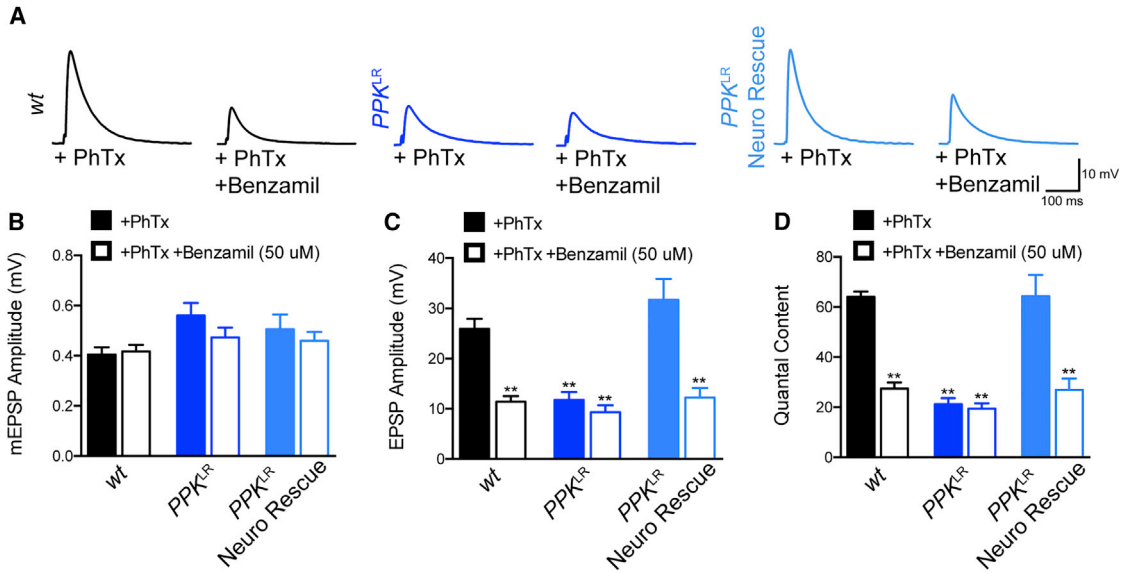

Figure 5. PPK1 Is Necessary for the Benzamil-Sensitive Induction of PHP

(A) Representative traces for indicated genotypes and treatments. All preparations were pre-incubated for 10 min in PhTx (+PhTx). After PhTx incubation, mEPSP and EPSP were recorded from muscle 6. Benzamil was applied to the preparations through perfusion for 10 min (+benzamil), and mEPSP and EPSP were recorded a second time from the same muscle.

(B) Quantification of mEPSP for indicated genotypes and treatments for conditions shown in (A).

(C) Quantification of average ESPS as in (B). (**$p < 0.001$; Student's t test, two tailed).

(D) Quantification of average quantal content as in (B). (**$p < 0.001$; Student's t test, two tailed).

Data are presented as average ± SEM.

demonstrated that age-related motor defects can be observed in other mutant backgrounds at 20 days post-eclosion (Liu et al., 2015), so we are within an appropriate time window to observe a phenotype. Finally, by assessing behavior at mid-life, animal viability is not yet a confound.

We compared three genotypes: wild-type controls; *PPK1^{LR}* mutants; and animals in which *PPK1* expression is knocked down selectively in motoneurons using *OK371-Gal4*-driving expression of *UAS-PPK1-RNAi*. All three genotypes showed robust negative geotaxis when assayed one day after adult eclosion. When re-tested 30 days post-eclosion, the *PPK1^{LR}* mutants revealed a consistent deficit in negative geotaxis compared to wild-type. However, motoneuron knockdown of *PPK1*, sufficient to block PHP, had no effect on negative geotaxis at this time point. From these data, we conclude that loss of PPK1 in a tissue other than motoneurons contributes to an age-related decline in motor function. This cannot be attributed to PHP at the neuromuscular junction. It is possible that there is an age-related induction of PHP within the CNS that is PPK1 dependent. Alternatively, the loss of PPK1 in peripheral sensory neurons could impair sensory feedback, unrelated to homeostatic plasticity, and create an age-dependent decline in motor function.

DISCUSSION

Deg/ENaC and acid-sensitive ion channel (ASIC) ion channels are expressed throughout the mammalian CNS and peripheral nervous system, being implicated in learning-related plasticity and the response to physiological stress (Du et al., 2014; Kreple et al., 2014; Cho and Askwith, 2008; Giraldez et al., 2013; but see Wu et al., 2013). But, given that ENaC channels have potent activities to control cellular physiology in tissues as diverse as the kidney, lung, and colonic epithelium, it seems likely that we are only scratching the surface with respect to ENaC and ASIC channel function in the nervous system. Furthermore, even in those systems where ENaC channels are a focus of significant research, there remains much to learn about the regulatory mechanisms that control channel expression, trafficking, and surface retention (Boscardin et al., 2016).

In this study, we define the subunit composition of a *Drosophila* ENaC channel and demonstrate that this channel may be the central effector that is responsible for the expression of PHP at the neuromuscular junction.

An Emerging Model for ENaC Channel Regulation during PHP

The ENaC channel that controls PHP appears to be subject to exquisite post-translational control. First, the channel is either prevented from reaching the plasma membrane or is rendered inactive under baseline conditions. Neither pharmacological inhibition of the channel (Younger et al., 2013) nor mutations of any of the three subunits influence baseline presynaptic release. Second, ENaC channel activity is induced in seconds to minutes at the isolated NMJ, implying that the channel is either rapidly transferred to the plasma membrane or is activated at that site (Younger et al., 2013). Third, PHP is a rheostat-like process, adjusting release to the precise level of GluR inhibition (Frank et al.,

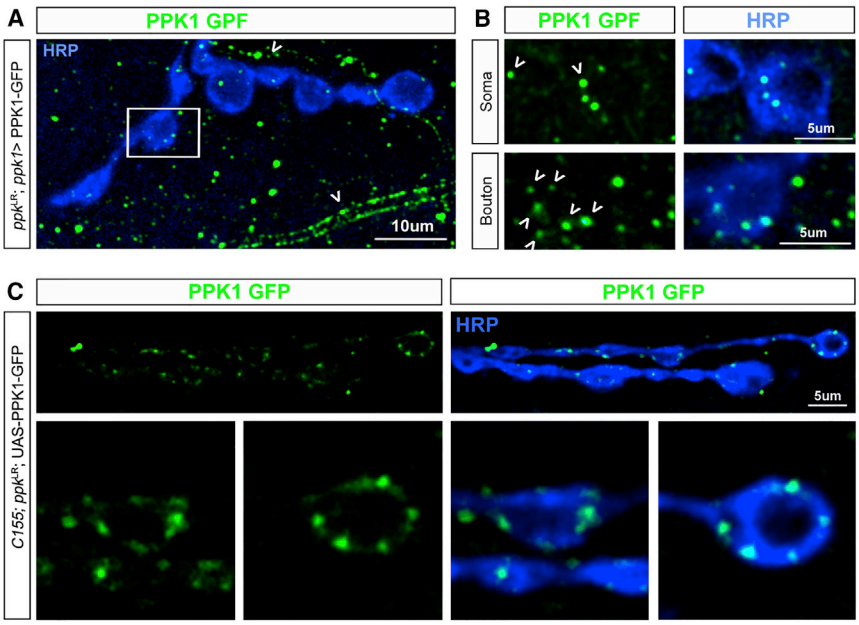

Figure 6. PPK1 Labeling Is Present at the *Drosophila* NMJ

(A) Expression of *ppk1-GFP* driven by the endogenous *ppk1* promoter in the ppk^{LR} mutant background (stained with anti-GFP). Images show the distribution of PPK1 protein visualized by anti-GFP staining (green). The motoneuron membrane is visualized by anti-HRP (blue). The white box highlights a region shown at higher magnification to the right. Arrowheads indicate trachea.

(B) Evidence that PPK protein (PPK1-GFP, green) can be visualized in a domain that overlaps presynaptic boutons (anti-HRP, blue) and the soma of motoneurons when PPK1-GFP (arrowhead) is expressed under the control of the *ppk1* promoter (*ppk1>PPK1-GFP*).

(C) Expression of *UAS-ppk1-GFP* in the ppk^{LR} mutant background shows localization of PPK1 protein (green) within the presynaptic terminal, defined by anti-HRP (blue). PPK1-GFP can be found at the periphery of individual boutons, at or near the membrane. All images are single confocal slices (~0.3 μm).

2006; Davis, 2013; Davis and Müller, 2015). The number of active ENaC channels on the plasma membrane must be precisely controlled to achieve this effect. Fourth, PHP can be sustained for weeks in *Drosophila* and decades in human (Davis and Müller, 2015). This implies, at least in *Drosophila*, that the number of active ENaC channels on the plasma membrane is precisely maintained. It will be of great interest to define the regulatory mechanisms that achieve such speed and precision.

By analogy with other systems, such as ENaC channel trafficking in the collecting duct of the kidney and the control of Glut4 surface expression, three types of post-translational control could be employed to regulate ENaC channel levels at the NMJ during PHP (Butterworth, 2010; Leto and Saltiel, 2012). First, there appears to be potent mechanisms to sequester intracellular ENaC channels, effectively preventing them from reaching the plasma membrane. The efficiency of this system is emphasized by the fact that overexpression of a hyper-active ENaC channel in *Drosophila* motoneurons is without effect (B.O.O. and G.W.D., unpublished data). Second, there must be efficient forward trafficking of ENaC channels to the plasma membrane to enable the rapid induction of PHP. Third, regulated recycling of the ENaC channels would be necessary to precisely maintain levels of the channel, given that channel residency is estimated to be as short as 20–30 min in other systems (Hanwell et al., 2002; Kabra et al., 2008). If these regulatory systems exist, the induction of PHP would require dis-inhibition of internal sequestration followed by the engagement of forward trafficking mechanisms (Butterworth, 2010; Leto and Saltiel, 2012). Alternatively, there could be mechanisms that restrict forward trafficking of ENaC channels to the membrane and these mechanisms would have to be disabled (Butterworth, 2010; Leto and Saltiel, 2012). The trigger for the induction of PHP might immediately act upon these processes. The feedback signaling system that tunes PHP to precise levels would presumably act upon the ENaC channel recycling mechanism, controlling the number of active ENaC channels on the synaptic plasma membrane. Together, these represent testable models for PHP induction and expression.

ENaC Channel Diversity based upon Co-assembly of Diverse PPK Subunits

The discovery that PPK1 is an essential component of a presynaptic ENaC channel expressed in motoneurons is surprising. Prior to this, PPK1 was thought to function primarily in the dendrites of peripheral multi-dendritic sensory neurons. *ppk1* is highly expressed in peripheral sensory neurons, and the *GFP ppk1*-promoter fusion line revealed high expression in these cells (Gorczyca et al., 2014). It is now apparent that *ppk1* is also expressed at lower levels in muscle, trachea, and motoneurons based on experiments with the *GFP ppk1*-promoter fusion line and the results of our genetic rescue and *ppk1-RNAi* experiments in motoneurons.

In peripheral sensory neurons, PPK1 has been shown to function as part of a mechanosensitive ion channel that is believed to be orthologous to *C. elegans* DEG/ENaC mechanosensors (Gorczyca et al., 2014; Guo et al., 2014). However, PPK1-containing channels that are expressed in *Drosophila* peripheral sensory neurons can also be gated by low pH, suggesting a parallel with ASICs that are expressed in mammalian peripheral sensory neurons and implicated in neuropathic pain (Boiko et al., 2012; Deval et al., 2011). There is, as yet, no evidence that PHP at the NMJ is induced by either mechanical or pH-dependent stimuli. PHP can be maximally induced in a relaxed NMJ preparation in the absence of action-potential-induced muscle contraction (Frank et al., 2006). Similarly, there is no evidence for low pH participating in the induction of PHP. Acid-sensitive currents are generally transient events with rapid inactivation, including those identified by *ppk1* in class IV multi-dendritic (md) sensory neurons (Boiko et al., 2012). This is in contrast to the requirement

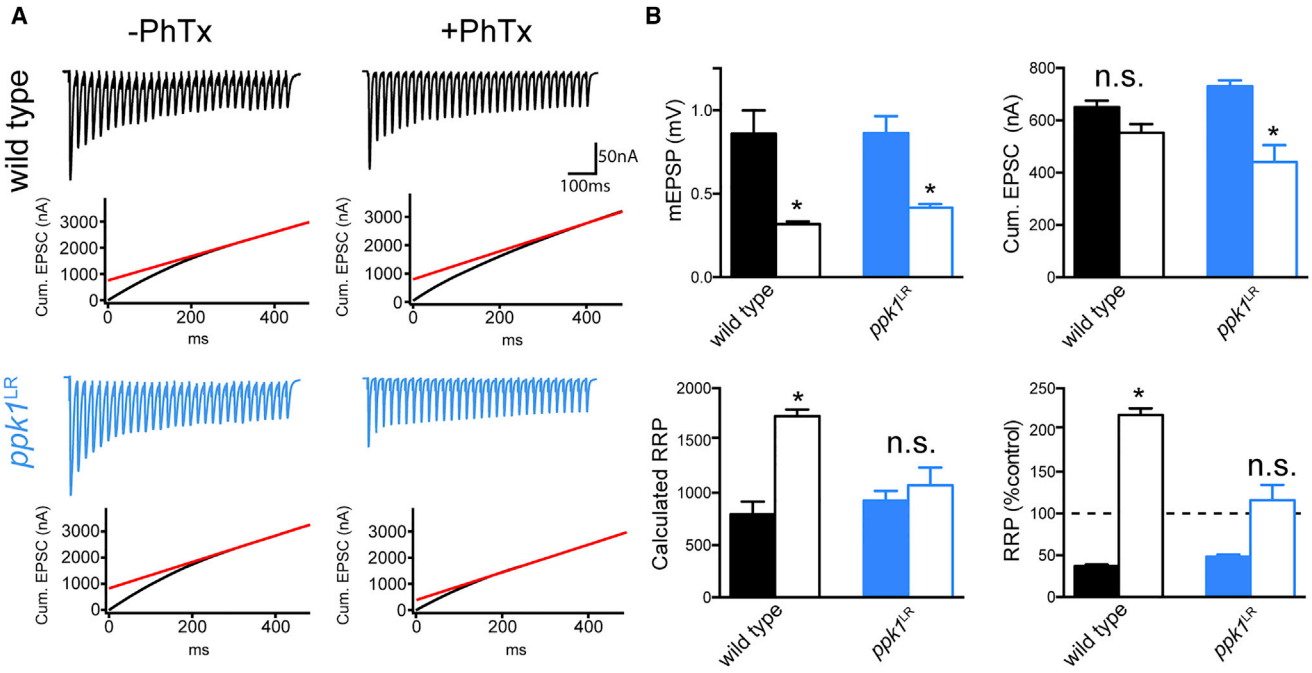

Figure 7. PPK1 Is Required for the Homeostatic Expansion of the Readily Releasable Pool of Synaptic Vesicles

(A) Representative traces from indicated genotypes in the absence and presence of PhTx. Voltage clamp recordings were performed at 1.5 mM $[Ca^{2+}]_e$, stimulation frequency 60 Hz.

(B) Averaged mEPSP, cumulative EPSC, and calculated RRP size for genotypes in (A). The change of the RRP in response to PhTx application is reported by averaged percent increase of the RRP in genotypes treated with PhTx compared to baseline physiology. (n.s. $p > 0.1$; asterisk $p < 0.002$; Student's t test). Data are presented as average ± SEM.

for a robust, sustained ENaC-mediated effect during the sustained expression of PHP, which can persist for weeks in adult *Drosophila* (Mahoney et al., 2014; Younger et al., 2013). Thus, the demonstration that PPK1 incorporates into DEG/ENaC channels with diverse physiological activities highlights the potential for tremendous DEG/ENaC channel diversity in *Drosophila*.

There are 31 PPK genes expressed in *Drosophila* that have been categorized into five subclasses (Zelle et al., 2013). Whereas it has been speculated that PPK genes co-assemble within subclasses, this does not seem to be the case given that PPK1 (subclass 5) appears to function with PPK11/16 (subclass 4) in motoneurons. There are other examples that suggest heterologous assembly, including evidence that PPK11 (subclass 4) functions with PPK19 (subclass 3; Liu et al., 2003) and that PPK23 (subclass 6) functions with PPK29 (subclass 1; Mast et al., 2014). As the subunit composition of ENaC channels in *Drosophila* is gradually resolved, we may discover the underlying rules for channel diversity and function base of PPK subunit composition (Zelle et al., 2013). Interestingly, there are hints that mammalian ASIC and non-acid-sensing ENaC channel subunits can co-assemble, thereby providing the potential for significant channel diversity in mammals as well (Meltzer et al., 2007).

EXPERIMENTAL PROCEDURES

Fly Stocks and Genetics

In all experiments, the w^{1118} strain was used as the wild-type control, including both male and females. Animals were maintained at 22°C. Progeny were raised at 25°C when performing rescue or overexpression experiments with the *GAL4/UAS* expression system. The following *Drosophila* stocks were used: ppk^{Minos} (*Mi{MIC}*$ppk^{MI04968}$; Bloomington 38075), ppk^{LR} (Boiko et al., 2012), *GluRIIA* (Petersen et al., 1997), *Df(2l)BSC240* (PPK deficiency; Bloomington 9715), *OK371-GAL4* (Mahr and Aberle, 2006), *C155-GAL4* (Lin and Goodman, 1994), *BG57-GAL4* (Budnik et al., 1996), *btl-GAL4* (Ohshiro and Saigo, 1997), *Actin-GAL4* (Gaumer et al., 2000), *UAS-ppk1-RNAi* (Xu et al., 2004), *UAS-ppk1-GFP* (Jan lab, UCSF), *ppk1>ppk1-EGFP* (Gorczyca et al., 2014), *UAS-ppk1-Flag* (Boiko et al., 2012), *UAS-ppk11-Flag*, *UAS-ppk11-αBt*, and *UAS-ppk16-Venus* (all generated for this study according to standard methods using Gateway technology and outsourced to BestGene for transgenesis).

Electrophysiology

Recordings were made from muscle 6 in abdominal segments 2 and 3 of third-instar larvae (Frank et al., 2006; Müller et al., 2012): hemolymph-like (HL3) saline (70 mM NaCl, 5 mM KCl, 10 mM $MgCl_2$, 10 mM $NaHCO_3$, 115 mM sucrose, 4.2 mM trehalose, and 5 mM HEPES). For acute pharmacological induction of PHP, larvae were incubated in PhTx (10–20 μM; Sigma-Aldrich) for 10 min before assaying synaptic transmission, according to previously published methods (Frank et al., 2006; Müller et al., 2012). EPSC train analyses were conducted using custom-written routines for Igor Pro 5.0 (Wavemetrics; Gaviño et al., 2015), and mEPSPs were analyzed using Mini Analysis 6.0.0.7 (Synaptosoft).

Anatomical Analysis

The following primary antibodies were used: anti-GFP 3E6 (1:500; mouse; Life Technologies); anti-GFP (1:100; rabbit; Thermo Scientific); anti-NC82 (1:100; mouse; Developmental Studies Hybridoma Bank); and anti-DLG (1:10,000; rabbit). Alexa-conjugated secondary (488 and 555) antibodies and Cy5-conjugated goat anti-HRP were used at 1:500 (Life Technologies; Molecular Probes). Larval preparations were mounted in Vectashield (Vector) and imaged

with an Axiovert 200 (Zeiss) inverted microscope, a 100× Plan Apochromat objective (1.4 not applicable [NA]), and a cooled charge-coupled device camera (Coolsnap HQ; Roper). Slidebook 5.0 Intelligent Imaging Innovations (3I) software was used to capture, process, and analyze images. Motor neuron cell bodies located in the *Drosophila* CNS were imaged with a Yokagawa CSU22 spinning disk confocal with a 60× oil objective (Nikon).

Biochemistry and Western Blot

Western blots of PPK1 protein levels using anti-PPK1 (1:3,000 rabbit; Gorczyca et al., 2014) in wild-type and *GluRIIA* were performed by dissecting three brains from each genotype and placing in sample buffer for cell lysis. Samples were boiled for 10 min and run on a NuPage 4%–12% Bis-Tris protein gel (Life Technologies). After protein transfer to a cellulous membrane (Bio-Rad), PPK1 was blotted with affinity-purified PPK1 antibody (rabbit) and anti-B-tubulin (rabbit). Band intensities were analyzed with ImageJ.

The co-immunoprecipitation (coIP) of PPK channel subunits was performed as follows. *UAS-ppk16-Venus* and *UAS-ppk11-FLAG* were expressed in vivo with the ubiquitous *Actin-GAL4* driver, and immunoprecipitations were performed using whole larva cell lysate with anti-GFP-3E6 (1:500; mouse; Life Technologies) and protein G beads. Endogenous PPK1 was immunoprecipitated using whole larva cell lysate with anti-PPK1 (2 μg/μL; rabbit) and protein A beads.

UAS-ppk16-Venus, *UAS-ppk1-FLAG*, and *UAS-ppk11-αBt* were expressed in vivo with the ubiquitous *Actin-GAL4* driver, and immunoprecipitation of PPK-Flag was performed with anti-FLAG (2 μg/μL; mouse; Sigma-Aldrich). Separate western blots were performed from the pull-down sample, where anti-GFP (mouse; clone N86/8; UC Davis/NIH NeuroMab Facility), anti-FLAG (Sigma-Aldrich), α-bungarotoxin, Alexa Fluor conjugate (Thermo Fisher Scientific), and anti-PPK1 antibodies were used to blot for each protein of interest. All protein detection was performed with HRP substrate Peirce Chemiluminescent (Life Technologies) or fluorophore detection.

SUPPLEMENTAL INFORMATION

Supplemental Information includes two figures and one table and can be found with this article online at http://dx.doi.org/10.1016/j.celrep.2017.07.074.

AUTHOR CONTRIBUTIONS

M.A.Y. performed the screen in Figure 1. B.O.O. conducted the remainder of experiments inclusive of data collection and analysis. D.G. and Y.-N.J. provided unpublished reagents and provided feedback on the manuscript text. B.O.O. and G.W.D. wrote the text.

ACKNOWLEDGMENTS

We thank Ozgur Genc and Ryan Jones for comments on the manuscript. We thank Amy Tong for technical help. This work was supported by NIH grants R01NS39313 and R35NS097212 (to G.W.D.), and R37NS040929 (to Y.-N.J.).

Received: January 7, 2017
Revised: April 10, 2017
Accepted: July 25, 2017
Published: August 22, 2017

REFERENCES

Anantharam, A., and Palmer, L.G. (2007). Determination of epithelial Na+ channel subunit stoichiometry from single-channel conductances. J. Gen. Physiol. *130*, 55–70.

Askwith, C.C., Cheng, C., Ikuma, M., Benson, C., Price, M.P., and Welsh, M.J. (2000). Neuropeptide FF and FMRFamide potentiate acid-evoked currents from sensory neurons and proton-gated DEG/ENaC channels. Neuron *26*, 133–141.

Askwith, C.C., Wemmie, J.A., Price, M.P., Rokhlina, T., and Welsh, M.J. (2004). Acid-sensing ion channel 2 (ASIC2) modulates ASIC1 H+-activated currents in hippocampal neurons. J. Biol. Chem. *279*, 18296–18305.

Boiko, N., Kucher, V., Stockand, J.D., and Eaton, B.A. (2012). Pickpocket1 is an ionotropic molecular sensory transducer. J. Biol. Chem. *287*, 39878–39886.

Boscardin, E., Alijevic, O., Hummler, E., Frateschi, S., and Kellenberger, S. (2016). The function and regulation of acid-sensing ion channels (ASICs) and the epithelial Na(+) channel (ENaC): IUPHAR Review 19. Br. J. Pharmacol. *173*, 2671–2701.

Brusich, D.J., Spring, A.M., and Frank, C.A. (2015). A single-cross, RNA interference-based genetic tool for examining the long-term maintenance of homeostatic plasticity. Front. Cell. Neurosci. *9*, 107.

Budnik, V., Koh, Y.H., Guan, B., Hartmann, B., Hough, C., Woods, D., and Gorczyca, M. (1996). Regulation of synapse structure and function by the Drosophila tumor suppressor gene dlg. Neuron *17*, 627–640.

Butterworth, M.B. (2010). Regulation of the epithelial sodium channel (ENaC) by membrane trafficking. Biochim. Biophys. Acta *1802*, 1166–1177.

Chalfie, M. (2009). Neurosensory mechanotransduction. Nat. Rev. Mol. Cell Biol. *10*, 44–52.

Chen, X., and Chalfie, M. (2015). Regulation of mechanosensation in C. elegans through ubiquitination of the MEC-4 mechanotransduction channel. J. Neurosci. *35*, 2200–2212.

Chen, Y., Bharill, S., Isacoff, E.Y., and Chalfie, M. (2015). Subunit composition of a DEG/ENaC mechanosensory channel of Caenorhabditis elegans. Proc. Natl. Acad. Sci. USA *112*, 11690–11695.

Cho, J.-H., and Askwith, C.C. (2008). Presynaptic release probability is increased in hippocampal neurons from ASIC1 knockout mice. J. Neurophysiol. *99*, 426–441.

Cull-Candy, S.G., Miledi, R., Trautmann, A., and Uchitel, O.D. (1980). On the release of transmitter at normal, myasthenia gravis and myasthenic syndrome affected human end-plates. J. Physiol. *299*, 621–638.

Davis, G.W. (2013). Homeostatic signaling and the stabilization of neural function. Neuron *80*, 718–728.

Davis, G.W., and Müller, M. (2015). Homeostatic control of presynaptic neurotransmitter release. Annual Review of Physiology *77*, 251–270.

Deval, E., Noël, J., Gasull, X., Delaunay, A., Alloui, A., Friend, V., Eschalier, A., Lazdunski, M., and Lingueglia, E. (2011). Acid-sensing ion channels in postoperative pain. J. Neurosci. *31*, 6059–6066.

Dickman, D.K., and Davis, G.W. (2009). The schizophrenia susceptibility gene dysbindin controls synaptic homeostasis. Science *326*, 1127–1130.

Du, J., Reznikov, L.R., Price, M.P., Zha, X.M., Lu, Y., Moninger, T.O., Wemmie, J.A., and Welsh, M.J. (2014). Protons are a neurotransmitter that regulates synaptic plasticity in the lateral amygdala. Proc. Natl. Acad. Sci. USA *111*, 8961–8966.

Firsov, D., Gautschi, I., Merillat, A.M., Rossier, B.C., and Schild, L. (1998). The heterotetrameric architecture of the epithelial sodium channel (ENaC). EMBO J. *17*, 344–352.

Frank, C.A., Kennedy, M.J., Goold, C.P., Marek, K.W., and Davis, G.W. (2006). Mechanisms underlying the rapid induction and sustained expression of synaptic homeostasis. Neuron *52*, 663–677.

Gaumer, S., Guénal, I., Brun, S., Théodore, L., and Mignotte, B. (2000). Bcl-2 and Bax mammalian regulators of apoptosis are functional in Drosophila. Cell Death Differ. *7*, 804–814.

Gaviño, M.A., Ford, K.J., Archila, S., and Davis, G.W. (2015). Homeostatic synaptic depression is achieved through a regulated decrease in presynaptic calcium channel abundance. eLife *4*, e05473.

Giraldez, T., Domínguez, J., and Alvarez de la Rosa, D. (2013). ENaC in the brain–future perspectives and pharmacological implications. Curr. Mol. Pharmacol. *6*, 44–49.

Goodman, M.B., Ernstrom, G.G., Chelur, D.S., O'Hagan, R., Yao, C.A., and Chalfie, M. (2002). MEC-2 regulates C. elegans DEG/ENaC channels needed for mechanosensation. Nature *415*, 1039–1042.

Gorczyca, D.A., Younger, S., Meltzer, S., Kim, S.E., Cheng, L., Song, W., Lee, H.Y., Jan, L.Y., and Jan, Y.N. (2014). Identification of Ppk26, a DEG/ENaC

channel functioning with Ppk1 in a mutually dependent manner to guide locomotion behavior in Drosophila. Cell Rep. *9*, 1446–1458.

Guo, Y., Wang, Y., Wang, Q., and Wang, Z. (2014). The role of PPK26 in Drosophila larval mechanical nociception. Cell Rep. *9*, 1183–1190.

Hanwell, D., Ishikawa, T., Saleki, R., and Rotin, D. (2002). Trafficking and cell surface stability of the epithelial Na+ channel expressed in epithelial Madin-Darby canine kidney cells. J. Biol. Chem. *277*, 9772–9779.

Harris, N., Braiser, D.J., Dickman, D.K., Fetter, R.D., Tong, A., and Davis, G.W. (2015). The innate immune receptor PGRP-LC controls presynaptic homeostatic plasticity. Neuron *88*, 1157–1164.

Hill, A., Zheng, X., Li, X., McKinney, R., Dickman, D., and Ben-Shahar, Y. (2017). The Drosophila postsynaptic DEG/ENaC channel ppk29 contributes to excitatory neurotransmission. J. Neurosci. *37*, 3171–3180.

Kabra, R., Knight, K.K., Zhou, R., and Snyder, P.M. (2008). Nedd4-2 induces endocytosis and degradation of proteolytically cleaved epithelial Na+ channels. J. Biol. Chem. *283*, 6033–6039.

Kim, S.H., and Ryan, T.A. (2010). CDK5 serves as a major control point in neurotransmitter release. Neuron *67*, 797–809.

Kosari, F., Sheng, S., Li, J., Mak, D.O.D., Foskett, J.K., and Kleyman, T.R. (1998). Subunit stoichiometry of the epithelial sodium channel. J. Biol. Chem. *273*, 13469–13474.

Kreple, C.J., Lu, Y., Taugher, R.J., Schwager-Gutman, A.L., Du, J., Stump, M., Wang, Y., Ghobbeh, A., Fan, R., Cosme, C.V., et al. (2014). Acid-sensing ion channels contribute to synaptic transmission and inhibit cocaine-evoked plasticity. Nat. Neurosci. *17*, 1083–1091.

Leto, D., and Saltiel, A.R. (2012). Regulation of glucose transport by insulin: traffic control of GLUT4. Nat. Rev. Mol. Cell Biol. *13*, 383–396.

Lin, D.M., and Goodman, C.S. (1994). Ectopic and increased expression of Fasciclin II alters motoneuron growth cone guidance. Neuron *13*, 507–523.

Lin, H., Mann, K.J., Starostina, E., Kinser, R.D., and Pikielny, C.W. (2005). A Drosophila DEG/ENaC channel subunit is required for male response to female pheromones. Proc. Natl. Acad. Sci. USA *102*, 12831–12836.

Liu, L., Johnson, W.A., and Welsh, M.J. (2003). Drosophila DEG/ENaC pickpocket genes are expressed in the tracheal system, where they may be involved in liquid clearance. Proc. Natl. Acad. Sci. USA *100*, 2128–2133.

Liu, H., Han, M., Li, Q., Zhang, X., Wang, W.A., and Huang, F.D. (2015). Automated rapid iterative negative geotaxis assay and its use in a genetic screen for modifiers of Aβ(42)-induced locomotor decline in Drosophila. Neurosci. Bull. *31*, 541–549.

Mahoney, R.E., Rawson, J.M., and Eaton, B.A. (2014). An age-dependent change in the set point of synaptic homeostasis. J. Neurosci. *34*, 2111–2119.

Mahr, A., and Aberle, H. (2006). The expression pattern of the Drosophila vesicular glutamate transporter: a marker protein for motoneurons and glutamatergic centers in the brain. Gene Expr. Patterns *6*, 299–309.

Marder, E., and Goaillard, J.-M. (2006). Variability, compensation and homeostasis in neuron and network function. Nat. Rev. Neurosci. *7*, 563–574.

Mast, J.D., De Moraes, C.M., Alborn, H.T., Lavis, L.D., and Stern, D.L. (2014). Evolved differences in larval social behavior mediated by novel pheromones. eLife *3*, e04205.

Mauthner, S.E., Hwang, R.Y., Lewis, A.H., Xiao, Q., Tsubouchi, A., Wang, Y., Honjo, K., Skene, J.H., Grandl, J., and Tracey, W.D., Jr. (2014). Balboa binds to pickpocket in vivo and is required for mechanical nociception in Drosophila larvae. Curr. Biol. *24*, 2920–2925.

Meltzer, R.H., Kapoor, N., Qadri, Y.J., Anderson, S.J., Fuller, C.M., and Benos, D.J. (2007). Heteromeric assembly of acid-sensitive ion channel and epithelial sodium channel subunits. J. Biol. Chem. *282*, 25548–25559.

Müller, M., Liu, K.S.Y., Sigrist, S.J., and Davis, G.W. (2012). RIM controls homeostatic plasticity through modulation of the readily-releasable vesicle pool. J. Neurosci. *32*, 16574–16585.

Müller, M., Genç, Ö., and Davis, G.W. (2015). RIM-binding protein links synaptic homeostasis to the stabilization and replenishment of high release probability vesicles. Neuron *85*, 1056–1069.

Ohshiro, T., and Saigo, K. (1997). Transcriptional regulation of breathless FGF receptor gene by binding of TRACHEALESS/dARNT heterodimers to three central midline elements in Drosophila developing trachea. Development *124*, 3975–3986.

Penney, J., Tsurudome, K., Liao, E.H., Elazzouzi, F., Livingstone, M., Gonzalez, M., Sonenberg, N., and Haghighi, A.P. (2012). TOR is required for the retrograde regulation of synaptic homeostasis at the Drosophila neuromuscular junction. Neuron *74*, 166–178.

Petersen, S.A., Fetter, R.D., Noordermeer, J.N., Goodman, C.S., and DiAntonio, A. (1997). Genetic analysis of glutamate receptors in Drosophila reveals a retrograde signal regulating presynaptic transmitter release. Neuron *19*, 1237–1248.

Schneggenburger, R., Meyer, A.C., and Neher, E. (1999). Released fraction and total size of a pool of immediately available transmitter quanta at a calyx synapse. Neuron *23*, 399–409.

Sherwood, T.W., Lee, K.G., Gormley, M.G., and Askwith, C.C. (2011). Heteromeric acid-sensing ion channels (ASICs) composed of ASIC2b and ASIC1a display novel channel properties and contribute to acidosis-induced neuronal death. J. Neurosci. *31*, 9723–9734.

Thanawala, M.S., and Regehr, W.G. (2013). Presynaptic calcium influx controls neurotransmitter release in part by regulating the effective size of the readily releasable pool. J. Neurosci. *33*, 4625–4633.

Toda, H., Zhao, X., and Dickson, B.J. (2012). The Drosophila female aphrodisiac pheromone activates ppk23(+) sensory neurons to elicit male courtship behavior. Cell Rep. *1*, 599–607.

Turrigiano, G.G. (2008). The self-tuning neuron: synaptic scaling of excitatory synapses. Cell *135*, 422–435.

Wang, T., Hauswirth, A.G., Tong, A., Dickman, D.K., and Davis, G.W. (2014). Endostatin is a trans-synaptic signal for homeostatic synaptic plasticity. Neuron *83*, 616–629.

Wang, X., Pinter, M.J., and Rich, M.M. (2016). Reversible recruitment of a homeostatic reserve pool of synaptic vesicles underlies rapid homeostatic plasticity of quantal content. J. Neurosci. *36*, 828–836.

Wu, P.-Y., Huang, Y.-Y., Chen, C.-C., Hsu, T.-T., Lin, Y.-C., Weng, J.-Y., Chien, T.-C., Cheng, l.H., and Lien, C.-C. (2013). Acid-sensing ion channel-1a is not required for normal hippocampal LTP and spatial memory. J. Neurosci. *33*, 1828–1832.

Xu, K., Bogert, B.A., Li, W., Su, K., Lee, A., and Gao, F.-B. (2004). The fragile X-related gene affects the crawling behavior of Drosophila larvae by regulating the mRNA level of the DEG/ENaC protein pickpocket1. Curr. Biol. *14*, 1025–1034.

Younger, M.A., Müller, M., Tong, A., Pym, E.C., and Davis, G.W. (2013). A presynaptic ENaC channel drives homeostatic plasticity. Neuron *79*, 1183–1196.

Zelle, K.M., Lu, B., Pyfrom, S.C., and Ben-Shahar, Y. (2013). The genetic architecture of degenerin/epithelial sodium channels in Drosophila. G3 (Bethesda) *3*, 441–450.

Zhao, C., Dreosti, E., and Lagnado, L. (2011). Homeostatic synaptic plasticity through changes in presynaptic calcium influx. J. Neurosci. *31*, 7492–7496.